[Papers in Palaeontology, 2023, e1530]

Elucidating the morphology and ecology of *Eoandromeda octobrachiata* from the Ediacaran of South Australia

by TORY L. BOTHA[1,*], EMMA SHERRATT[1], MARY L. DROSER[2], JIM G. GEHLING[3] *and* DIEGO C. GARCÍA-BELLIDO[1,3]

[1]School of Biological Sciences, Faculty of Sciences, Engineering & Technology, University of Adelaide, North Terrace, Adelaide, South Australia, Australia; tory.botha@adelaide.edu.au

[2]Department of Earth & Planetary Sciences, University of California at Riverside, Riverside, California, USA

[3]Earth Sciences Section, South Australian Museum, North Terrace, Adelaide, South Australia, Australia

*Corresponding author

Typescript received 11 December 2022; accepted in revised form 27 July 2023

Abstract: *Eoandromeda octobrachiata* is a poorly understood Ediacaran organism, with spiral octoradial arms, found in South Australia and South China. The informal Nilpena member of the Rawnsley Quartzite, Flinders Ranges in South Australia preserves more than 200 specimens of *Eoandromeda*. Here we use the novel application of rotational geometric morphometrics together with palaeoenvironmental information to provide a better insight into their palaeobiology and ecology, and to address conflicting hypotheses regarding mode of life and taxonomic affinity. We find that *Eoandromeda* probably had a radially symmetrical shape in life, was cone shaped and had a high relief off the microbial mat. Analysis of the symmetric and asymmetric shape components showed that they deform strongly in the direction of palaeocurrent, therefore they are thought to be made of a flexible material. Almost all specimens are compressed flat. Specimens that appear to have not fully collapsed support the idea that *Eoandromeda* was probably cone shaped and suggest that they possibly collapsed spirally. Our shape analysis, along with observed morphological features, support a benthic rather than pelagic mode of life. Morphological and ecological inconsistencies do not fully support the hypothesis of a Ctenophora taxonomic affinity.

Key words: Ediacara, *Eoandromeda*, South Australia, morphometrics, benthic.

THE Ediacaran period spanned 94 myr (635–539 Ma; Cohen *et al.* 2013, v2022/10) and included the first record of complex, macroscopic, multicellular life. The Ediacara biota is grouped into three assemblages: the Avalon (*c.* 575–565 Ma), White Sea (*c.* 558–555 Ma) and Nama (*c.* 549–541 Ma). South Australian fossil sites contain the most morphologically and taxonomically diverse White Sea assemblage (Droser & Gehling 2015; Coutts *et al.* 2016; Droser *et al.* 2019). These fossils occur in the Ediacara Member throughout the Flinders Ranges of South Australia, with the upper metres comprising the informal Nilpena Member found only at Nilpena Ediacara National Park (NENP).

Eoandromeda octobrachiata is an enigmatic soft-bodied, octoradial spiral organism found with contrasting preservation in two locations globally: carbonaceous compressions in the Doushantuo Formation (South China) (Tang *et al.* 2008) and negative impressions (external moulds) in the informal Nilpena member of the Rawnsley Quartzite, South Australia (Zhu *et al.* 2008). The current hypothesis for the taxonomic affinity is Ctenophora (Tang *et al.* 2011a; Wang *et al.* 2020). The ecology of *Eoandromeda* is uncertain and has been proposed as both pelagic (Wang *et al.* 2020) and benthic (Zhu *et al.* 2008). Excavation of extensive fossil surfaces with *in situ* preservation of Ediacara taxa, including nearly 200 specimens of *Eoandromeda* at NENP, east of the Flinders Ranges provides an opportunity to examine *in situ Eoandromeda* in a sedimentological context.

Here we investigate the palaeobiology and ecology of *Eoandromeda* and address the conflicting life mode hypotheses through the novel application of a shape analysis approach, rotational geometric morphometrics (Savriama 2018). We estimate the shape in life and examine patterns of asymmetry across various fossil beds from NENP to understand how the shape of *Eoandromeda* is altered by differing burial conditions. Following these analyses, we assess how the shape changed with size to infer how *Eoandromeda* grew. Based upon all of the results and observations, we discuss the mode of life and taxonomic affinities.

GEOLOGICAL SETTING

The Adelaide Geosyncline is a north–south-oriented rift complex in South Australia dating from the

doi: 10.1002/spp2.1530

Neoproterozoic to the middle Cambrian (Preiss 2000). Deposits containing the Ediacaran biota occur in the Pound Subgroup (Fig. 1A) (Gehling *et al.* 2019). In the absence of absolute radiometric dates in the area, the age of the strata bearing Ediacara biota in South Australia is *c.* 555 Ma, based on dates from the Russian sites, which include *Dickinsonia* and *Kimberella* (Martin *et al.* 2000). The Pound Subgroup (Fig. 1A) consists of the red Bonney Sandstone disconformably overlain by the coarse felspathic Rawnsley Quartzite. The base of this Rawnsley Quartzite is the unfossiliferous Chace Quartzite Sandstone Member (Gehling 2000). The overlying fossiliferous Ediacara Sandstone Member cuts deep channels and canyon incisions into the Chace Quartzite Member, and in some cases into the Bonney Sandstone (Gehling 2000; Gehling & Droser 2012).

Overall, the Ediacara Member is a deltaic succession prograding northwestward, the resulting accommodation space provided by the canyons enabled the development of different facies (Gehling 2000; Gehling & Droser 2012, 2013). Recently, a new member has been informally described that caps the Rawnsley Quartzite: the Nilpena Sandstone member (Fig. 1B) (Gehling *et al.* 2019). This member is characterized by the presence of *Phyllozoon hanseni*, *Eoandromeda octobrachiata*, *Arkarua adami* and *Tribrachidium*. It is geographically restricted to the central Flinders Ranges, at both the NENP and some sections of the Heysen Range.

The *Eoandromeda* specimens used in this study occur at the NENP site in the Planar-Laminated & Rip-Up Sandstone Facies (J. Gehling, M. Droser & D. García-Bellido, pers. obs. 2020), which is interpreted to represent deposition below wave base with gravity and/or unidirectional flow, and deposition (Gehling & Droser 2013; Tarhan *et al.* 2017). Specimens occur on three beds at the NENP: WS-Parv (West Side *Parvancorina* bed), WS-Sub (West Side Sub bed) and LV-Eo (Lake View *Eoandromeda* bed) as well as on float pieces around the LV-Eo bed. These beds are not stratigraphically constrained with respect to each other but are in the same facies succession. The WS-Parv bed is fine grained, with evidence of a strong unidirectional current as indicated by tool marks and oriented frond stalks, and is dominated by *Parvancorina* with only 15 *Eoandromeda* specimens (Droser *et al.* 2019). The WS-Sub bed is dominated by *Coronacollina* (Droser *et al.* 2019) with 14 *Eoandromeda* specimens. There is a well-developed textured organic surface indicative of a mature organic mat (Droser *et al.* 2022). Oriented fronds indicate a unidirectional current but there is otherwise a lack of current indicators, suggesting that the

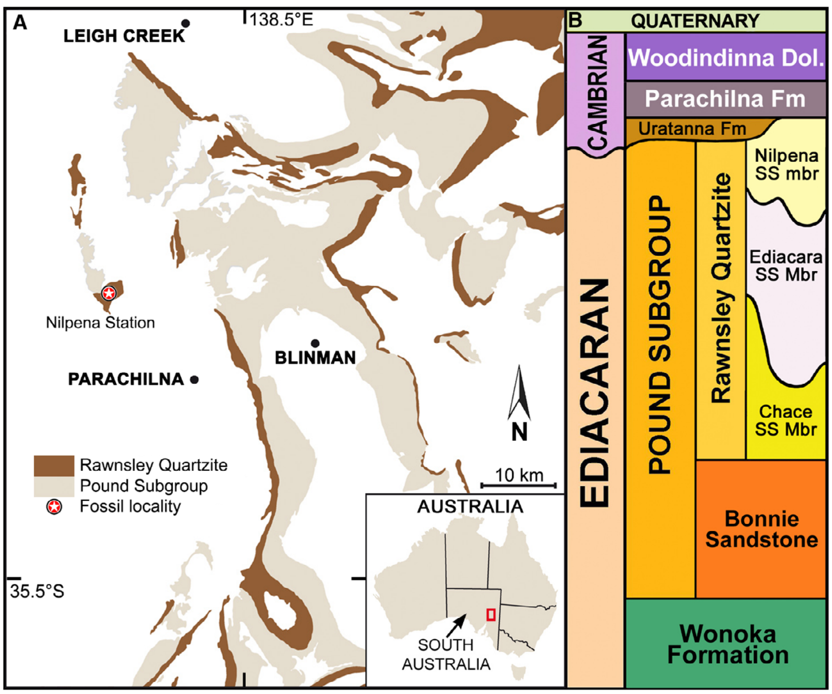

FIG. 1. A, map indicating the location of Nilpena Ediacara National Park, Flinders Ranges, South Australia, the Pound Subgroup (part of geosyncline) and the Rawnsley Quartzite, which contains the fossiliferous members. B, schematic sequence with the new informally described Nilpena Sandstone (SS) member shown above the Ediacara Sandstone member. Both modified from Turner *et al.* (2021).

burial event was not as strong as in the WS-Parv bed. Finally, the LV-Eo bed is dominated by *Eoandromeda* (*c.* 52 specimens), it has a very well developed textured organic surface and no evidence of current impact on the fossils.

MATERIAL AND METHOD

Specimens from NENP located in the field and in the South Australian Museum collections (SAMA) comprise the 230 *Eoandromeda* used in this study (Table 1; Fig. 2). However, because not all specimens are complete, the total number of specimens available is 95. Three-dimensional (3D) surfaces of these specimens were captured using the HDI Compact C506 and 3Shape TROIS 4 Intraoral 3D laser scanners (accuracies reported to 12 μm and *c.* 5 μm, respectively). Scans were prepared using the FlexScan3D and TRIOS Design Studio software (correspondingly) and processed (landmarked and measured) in the MeshLab software (Cignoni *et al.* 2008).

First, arm width was measured at the maximum width to determine whether there was one or more dominant arm/s, to orient the specimens for landmarking. Arm width was chosen given that deformation impeded the view of each arm's full length. Cross-sections of scans were visually assessed, and a wavelength pattern of the arms was determined (Fig. S1). Accordingly, arm width measurements were taken from valley to valley on scans of the complete specimens only.

Eoandromeda's form was captured using landmark-based geometric morphometrics (Bookstein 1991; Mitteroecker & Gunz 2009). Due to the varying length of the arms, to adequately capture the bends, each arm was initially landmarked with a different number of landmarks along a linear curve. Then, all curves were standardized to ensure that each arm had seven landmarks by resampling landmarks equally distantly along the length of the curve by a routine written in R using the digit.curves function in geomorph (Fig. 3A). All analyses were conducted in the R Statistical Environment v4.0.3 (R Core Team 2013) using Morpho v2.9 (Schlager 2017), geomorph v4.0.1 (Adams *et al.* 2021), shapes v1.2.5 (Dryden 2019), ggplot2 v3.3.5 (Wickham 2016) and abind v1.4.5 (Plate & Heiberger 2016) unless otherwise stated.

To account for the rotational symmetry, the landmark data were rotated and relabelled to create eight transformed copies for each specimen using R functions in Savriama (2018) (each specimen has eight possible configurations; Fig. 3A). All transformed copies underwent generalized Procrustes analysis, which superimposes all the landmark configurations and removes translation, scale and rotation (Rohlf & Slice 1990) using the procSym function in Morpho. The resulting Procrustes coordinates are averaged across all configurations to produce a consensus (mean) shape (Fig. 3B) to estimate *Eoandromeda*'s shape in life.

To address how shape and asymmetry varied between the beds, the Procrustes coordinates were subset by bed and ordinated by principal component analysis (PCA) using the gm.prcomp function in geomorph. In rotational geometric morphometrics, PCA decomposes the data into symmetric and asymmetric axes. Shape deformation graphs corresponding to each principal component (PC) axis were plotted to determine differences in asymmetry patterns across the beds, and enable inference of their palaeoenvironmental conditions (Fig. 3C). Additionally, incomplete specimens from the field were categorized on a scale of 0 (perfectly symmetrical) to 3 (completely offset) to ensure analysis of all available specimens (Fig. S2). Furthermore, specimen offset angles were measured against true north for all three beds and compared with palaeocurrent proxies (from Paterson *et al.* (2017) for WS-Parv) to explore the effect of current strength during burial on their shape. Only 35 of the 52 specimens available on the LV-Eo bed were sufficiently complete to measure.

To evaluate *Eoandromeda* growth, the allometric relationship between shape and size for each bed was analysed using a multivariate regression (Loy *et al.* 1998; Monteiro 1999) implemented with the proc.D.lm function in geomorph. Size was taken as log-transformed centroid size (mm), where centroid size is calculated from the 3D landmarks as the square root of the sum of squared distances of a set of landmarks from their centroid (Bookstein 1991). The allometric relationship between the asymmetric shape components and size for all specimens was also analysed to investigate the correlation between deformation and size. To gain another perspective into their growth not captured by landmarks, the mean of linear measurements of the arm widths (per specimen) and of the arm lengths (per specimen)

TABLE 1. Number of *Eoandromeda octobrachiata* found in the field and number of landmarked specimens.

Specimen locations	No. specimens	Landmarked specimens
WS-Parv bed	15	10
WS-Sub bed	14	4
LV-Eo bed + Float	~170	74
SAMA collections	32	7
Total	~230	95

Eoandromeda bed (LV-Eo) and float pieces are combined given that they are from the same event layer (but do not form a contiguous bed).

FIG. 2. *Eoandromeda octobrachiata* from Nilpena Ediacara National Park, Flinders Ranges, South Australia. A, SAMA P42440. B, SAMA P44349. C, WS-Sub Bed 207S 420E. D, LV-Eo Bed 277S 129E. E, SAMA P58622. F, LV-Parv Bed 152S 576E. G–H, SAMA P49301. I–J, SAMA P49302. False coloured images are topographic heat maps of three-dimensional scans created in the R Statistical Environment v4.0.1 (R Core Team 2013), to better visualize the conical centre. Scale bars represent 1 cm.

was calculated. The variables were transformed using the log-shape ratios approach, in which each measurement is divided by size (calculated as the geometric mean of all measurements, or centroid size) and natural logarithm-transformed to obtain the shape variables (Mosimann 1970; Claude 2013). This method corrects for size while retaining the allometric shape variation (Klingenberg 2016). Ordinary least-squares linear regressions were performed on these shape variables and natural logarithm-transformed centroid size to test for allometry.

SYSTEMATIC PALAEONTOLOGY

Class, order & family unassigned

Genus EOANDROMEDA Tang *et al.*, 2008

Emended diagnosis. Soft-bodied spiral organism with eight arms radiating from a central part. Circular, quadrate to elongated in shape, with the centre sometimes offset to the side. Always spiral anticlockwise when viewed in a fossil bed as a negative hyporelief (external mould), however can spiral in both directions when viewed as a carbonaceous compression.

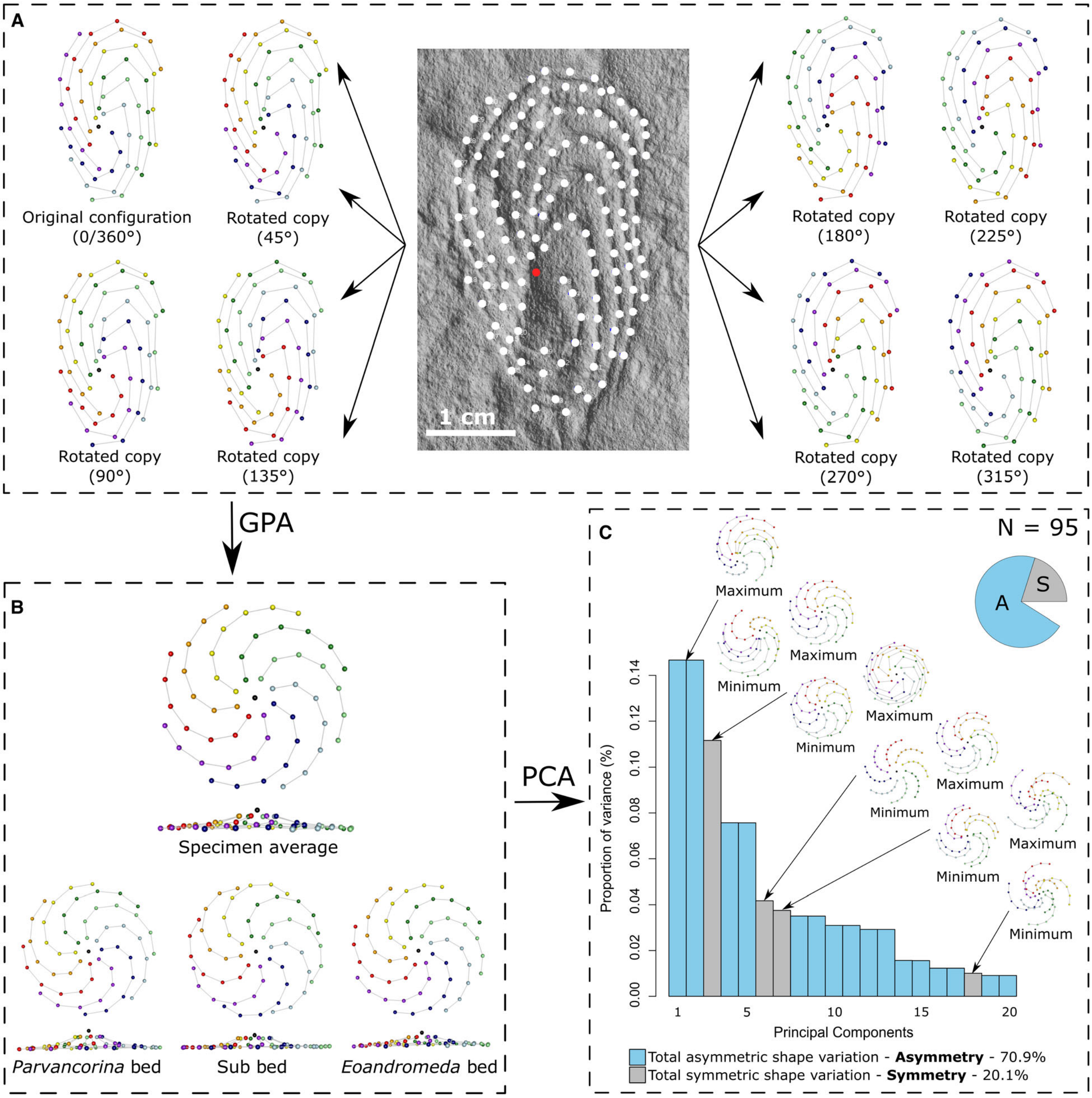

FIG. 3. Workflow for the shape analysis of *Eoandromeda octobrachiata*. A, original landmarked specimen (LV-Eo Bed 277S 129E) and its seven standardized rotated copies. B, consensus (mean) shape for all specimens and each bed. C, bar plot of the first 20 principal components (PCs); symmetrical components are identified as single PCs, asymmetrical components are paired PCs (arranged by the proportion of variance they explain); shape configuration graphs are given for key PCs, the shape of the minimum and maximum scores for the axis.

Type species. Eoandromeda octobrachiata Tang *et al*., 2008.

Remarks. Transverse bands appear on the arms of some of the specimens found in South China. After close re-examination of the specimens from South Australia, they were found to be absent despite their proposed presence in Zhu *et al*. (2008). A specimen was illustrated as having these structures (Zhu *et al*. 2008, fig. 2D), but it cannot be ruled out as an artefact of the sandstone grains. Bends or kinks seen in one arm are also seen in the neighbouring arms.

Eoandromeda octobrachiata Tang *et al*., 2008
Figure 2

1996 *Eilscaptichnus* Ding, Huang, Xiao & Hu *in* Ding *et al*., *nomen nudum*.

2008 *Eoandromeda octobrachiata* Tang *et al*., figs 2–3, pp. 29–33.
2008 *Eoandromeda octobrachiata* Tang *et al*.; Zhu *et al*., figs 1–2, pp. 868–869.
2009 *Eoandromeda octobrachiata* Tang *et al*.; Yin *et al*., fig. 2, pp. 423–430.
2009 *Eilscaptichnus* Ding *et al*.; Yin *et al*., fig. 1, p. 423.
2009 *Eoandromeda octobrachiata* Tang *et al*.; Tang *et al*., figs 2–4, pp. 547–549.
2011a *Eoandromeda octobrachiata* Tang *et al*.; Tang *et al*., figs 1–2, pp. 409–413.
2011b *Eoandromeda octobrachiata* Tang *et al*.; Tang *et al*., fig. 1, pp. 643–646.
2012 *Eoandromeda octobrachiata* Tang *et al*.; Tang, figs 3–4, pp. 724–727.
2012 *Eoandromeda octobrachiata* Tang *et al*.; Gehling & Droser, fig. 7, pp. 242–243.
2012 *Eoandromeda octobrachiata* Tang *et al*.; Narbonne *et al*., fig. 18.2–3, pp. 417–419.
2013 *Eoandromeda octobrachiata* Tang *et al*.; Gehling & Droser, table 1, fig. 2, pp. 448–450.
2013 *Eoandromeda octobrachiata* Tang *et al*.; Xiao *et al*., fig. 1, p. 1096.
2014 *Eoandromeda octobrachiata* Tang *et al*.; MacGabhann, fig. 1, pp. 56–59.
2016 *Eoandromeda octobrachiata* Tang *et al*.; Cunningham *et al*., fig. 3, pp. 4–7.
2017 *Eoandromeda octobrachiata* Tang *et al*.; Droser *et al*., fig. 1, p. 594.
2017 *Eoandromeda octobrachiata* Tang *et al*.; Zhu & Li, fig. 1, p. 1188.
2018 *Eoandromeda octobrachiata* Tang *et al*.; Zhou *et al*., fig. 2, p. 8.
2020 *Eoandromeda octobrachiata* Tang *et al*.; Wang *et al*., figs 2–4, 6, pp. 3–11.

Diagnosis. As for the genus (Tang *et al*. 2008, p. 33).

Holotype. JK05006, Institute of Geology, Chinese Academy of Geological Sciences (Tang *et al*. 2008, fig. 2A–G).

Material. Approximately 200 specimens located on three separate beds (WS-Parv, WS-Sub and LV-Eo) with additional specimens on float pieces around the LV-Eo bed.

Description. Eoandromeda octobrachiata is subcircular, quadrate or elongated, with a diameter ranging from 5 to 50 mm and arms that consistently spiral anticlockwise when viewed in the bed as a negative hyporelief (thus clockwise in life). When preserved as a carbonaceous compression, spiralling can occur in either direction (original stratigraphic orientation unknown). The arms tend to be long, tightly coiled, meeting proximally at a centre disc and tapering distally. This suggests that they were joined, forming a circle at the margin of the body (Fig. 2) that collapsed during burial. In some cases, the centre can be offset to the side (with the arms spread out to the side). Specifically for the carbonaceous compressions, in some specimens, transverse bands are visible along the arms (structures running perpendicular along the arms; Tang *et al*. 2011a, fig. 1A, C–F). The arms appear as lighter stains with the space between appearing darker (Tang *et al*. 2011a, 2011b). In a few specimens a central disc can be clearly seen, analogous to the central structure of the Australian material.

Occurrence. Upper Doushantuo black shales at the village of Wenghui, Jiangkou County, Guizhou Province, China, and Nilpena sandstone member at NENP, Flinders Ranges, South Australia, Australia.

SHAPE ANALYSIS

All specimens

Arm width measurements indicate that there was no arm wider than the others (Fig. S1), and thus *Eoandromeda* was established to have rotational symmetry of order 8. The consensus shape for all of the landmarked *Eoandromeda* specimens was symmetrical (with respect to rotational symmetry of order 8) with relatively loosely coiled arms (Fig. 3B). PCA of the Procrustes residuals yielded a total of 171 PCs. Only the first 20 PCs were used because they explain 90–95% of the total shape variation; PCs after this are negligible. Of those 20 PCs, *c*. 71% were asymmetrical and *c*. 20%, symmetrical (Fig. 3C). In a scatter plot of the PC axes, no significant grouping of shapes was observed (Fig. S3).

Two specimens in the SAMA collections appear not to have fully collapsed during or after burial (Fig. 2G–J). Specimens P49301 and P49302 (Fig. 2G–J) have a high-relief, conical centre, with straight arms, which suddenly spiral at the base of the conical centre. P49301 (Fig. 2G, H) has one side that has collapsed where the arms begin spiralling closer to the centre than observed in P49302 (Fig. 2I, J).

Individual beds

Consensus shapes for the WS-Parv, WS-Sub and LV-Eo beds are all symmetrical with arms becoming respectively more loosely coiled (Fig. 3B). On PCA, WS-Parv had 11% symmetric shape variation and 81% asymmetric shape variation (Fig. 4A). WS-Sub had 12% symmetric shape variation and 86% asymmetric shape variation (Fig. 4B). Finally, the LV-Eo bed + float had the highest proportion of symmetric shape variation at 19% and correspondingly the lowest asymmetric shape variation at 72% (Fig. 4C). WS-Parv has evidence of a strong prevailing palaeocurrent measured through felled fronds and tool marks (Paterson *et al*. 2017), and the measured offset angles of *Eoandromeda* were found to be strongly oriented with the current (Fig. 4A). Additionally, WS-Sub bed has evidence of a weaker current through felled fronds, and *Eoandromeda* was also found to be oriented in the general direction of that current (Fig. 4B). The LV-Eo bed does not show evidence of a current (Fig. 4C), which seems consistent with the orientation of *Eoandromeda* occurring in all directions. Categorizing of incomplete specimens followed similar trends (Fig. S2), with both the WS-Parv and WS-Sub beds having a higher proportion (80% and 93%, respectively) of the categories representing higher asymmetry (2–3) than the LV-Eo bed, which had the lowest proportion (53%).

Allometry

Multivariate regression of the symmetric component of shape for all landmarked specimens (Table 2) indicated that only 2.15% of shape change is associated with size ($p = 0.001$), where the general shape change is from loosely coiled with curved arms in small individuals to tightly coiled, angular arms in larger individuals (Fig. S4). Each bed follows the same trend of shape variation, with only 2.04% of shape variation being unique to each bed ($p = 0.001$). Asymmetric shape variation was not associated with size ($R^2 = 0$, $p = 1$).

Relatively strong linear allometric relationships were found for log arm width and log arm length versus log centroid size, and log arm length versus log width ($R^2 = 0.6517$, $R^2 = 0.5675$ and $R^2 = 0.4049$ respectively) with slope values of -0.4319, 0.2589 and -0.9995 (respectively; $p < 0.05$ for all) (Fig. 5).

DISCUSSION

Structure and shape in life

Given that radial organisms tend to be symmetrical (Manuel 2009; Hollo 2015), we hypothesize that *Eoandromeda* was as well. The consensus shape produced by the generalized Procrustes analysis is what is expected in life, after elimination of taphonomic distortion, which was perfectly radially symmetrical with respect to rotational symmetry of order 8 (Fig. 3B). Distinct patterns of asymmetry in the shape data were observed. Both WS-Parv and WS-Sub had a higher proportion of asymmetric shape components and a lower proportion of symmetric components than the LV-Eo bed (Fig. 4A–C, Fig. S2). A possible explanation for this is the current strength of the burial event. WS-Parv bed has evidence of a strong prevailing current (Paterson *et al.* 2017) and the WS-Sub bed has evidence of a weaker current through observed felled fronds, which could explain the higher asymmetry on those beds. The LV-Eo bed, however, has no evidence of a current, which is consistent with the lower proportion of asymmetry (Fig. 4C). The level of asymmetry observed on the LV-Eo bed, however, could be explained by the burial event itself. Multivariate regression of the asymmetric shape components against size showed that there is no asymmetric shape change with size (Table S1). Thus, the degree of asymmetry observed between beds was most probably not due to their size, but was more likely to be due to external factors such as current strength during burial. This is further supported by the orientation of deformation with the palaeocurrent on the WS-Parv and WS-Sub beds (Fig. 4D, E) and lack of orientation of deformation on the LV-Eo bed (Fig. 4F). Therefore, any asymmetry observed is interpreted as seemingly due to deformation as a result of palaeocurrent at the time of burial rather than asymmetry present in the body plan. Other taxa on the same beds do not show the same degree of deformation; consequently, it is hypothesized that *Eoandromeda* was most probably partially fluid-filled or made of a more flexible material with a high relief to be able to deform in the number of ways observed.

It is possible that *Eoandromeda* had a conical shape in life with a high relief off the microbial mat. The two specimens that appear to not have fully collapsed (Fig. 2G–J) suggest that *Eoandromeda* may have collapsed in a spiral, accommodating the tension in the arms by coiling, becoming more tightly coiled the more compacted they were. Therefore, the arms could have been more supportive in life, whether protein- or fluid-filled to support a conical shape and explain the compaction pattern. This is observed in the field, such that smaller specimens tend to have loosely coiled arms with very little relief in the centre, while larger specimens tend to have very tightly coiled arms with some relief maintained in the centre (more compaction required for the larger, higher/taller specimens). This shape pattern is also observed in the shape change in the multivariate regression (Fig. S4). However, there are only two specimens with this preservation, which were both found *ex situ* as an isolated piece, thus no confident claims can be made.

Growth

The hypotheses put forth by Wang *et al.* (2020) suggested that there were three distinct life stages based on an inflection in the regression slope of arm width versus size; juvenile (<10 mm diameter; not present in their dataset), adult (10–30 mm diameter) and senescent (>30 mm diameter) with a declining growth rate through the last two stages and a disproportionate increase of arm thickness

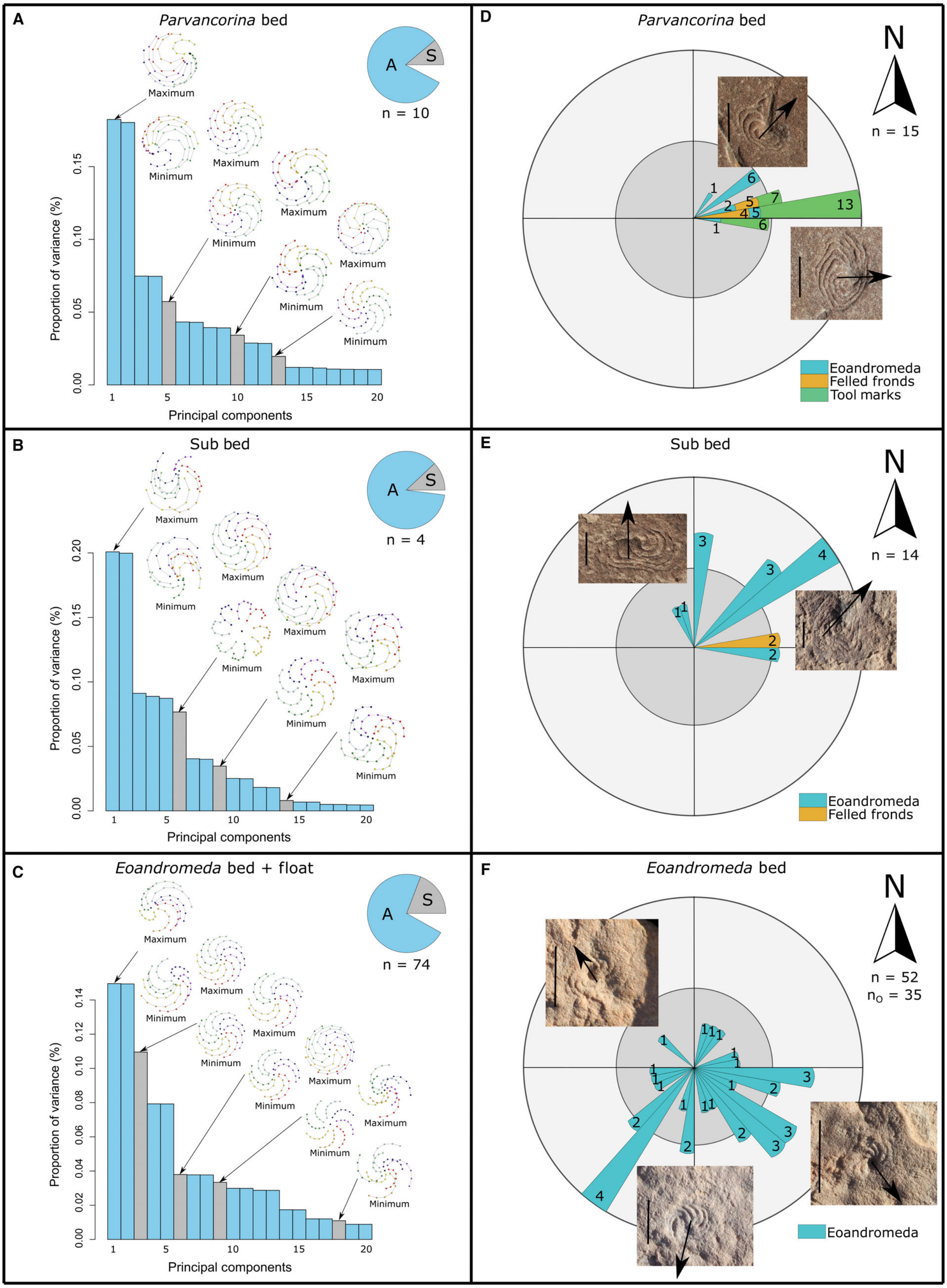
A
Parvancorina bed
A
S
n = 10
Maximum
Minimum
Proportion of variance (%)
Principal components
B
Sub bed
n = 4
C
Eoandromeda bed + float
n = 74
D
Parvancorina bed
N
n = 15
Eoandromeda
Felled fronds
Tool marks
E
Sub bed
n = 14
F
Eoandromeda bed
n = 52
n_O = 35

FIG. 4. Comparison of principal components (PCs) for each bed with current orientations. A–C, bar plots of the first 20 PCs for: A, WS-Parv bed; B, WS-Sub bed; C, LV-Eo bed; symmetrical components are identified as single PCs, asymmetrical components are paired PCs (arranged by the proportion of variance they explain); shape configuration graphs are given for key PCs, the shape of the minimum and maximum scores for the axis. D–F, offset angles of *Eoandromeda octobrachiata* (examples of offsetting illustrated) compared with palaeocurrent proxies: D, WS-Parv bed (proxies from Paterson *et al.* 2017); E, WS-Sub bed; F, LV-Eo bed (no evidence of a current).

TABLE 2. Multivariate regression results for shape change with size (first row), shape change by bed (second row) and shape change with size by bed (third row).

	d.f.	SS	MS	R^2	*F*	*Z*-score	Pr (>*F*)
log(size)	1	5.144	5.1438	0.02151	16.971	8.2061	0.001
Beds	3	4.879	1.6263	0.02041	5.3657	6.6225	0.001
log(size):beds	3	1.153	0.3843	0.00482	1.2679	1.1898	0.116
Residuals	752	227.927	0.3031	0.95326			
Total	759	239.103					

d.f., degrees of freedom; SS, sum of squares; MS, mean squares; Pr (>*F*), p-value. Level of significance set at p<0.05.

and rigidity compared to body size. In our analysis, the negative slope of the regression for arm width versus size lacks an inflection point (Fig. 5B), refuting the hypothesis of distinct life stages and a decline in growth rate from an initial positive incline. Furthermore, the value of the slope (-0.4319) indicates a negative allometric relationship: the width of the arms decreased relative to an increase in body size (Huxley & Teissierr 1936; Gould 1966; Klingenberg 2016). The regression of arm width versus arm length (-0.9995) also shows a negative allometric relationship, signifying that relative arm width also decreased as arm length increased. These results contradict the hypothesis that there is a disproportionate increase of arm thickness compared with body size.

However, the positive hypoallometric regression slope of arm length versus size (0.2589) indicates that arm length increased at a slower rate than body size (Huxley & Teissierr 1936; Gould 1966; Klingenberg 2016). The multivariate regression of all landmarked specimens found that only 2.151% of shape change is expected per unit of increase in size (Fig. S4). The allometric shape change was observed to be the arms becoming more tightly coiled with an increase in size. Therefore, *Eoandromeda* appears to primarily grow by increasing arm length as this is the only positive allometric relationship measured. The arms appear to grow in a spiral fashion, creating a more tightly coiled pattern in the larger specimens. It cannot be ruled out, however, that the tight coiling may have been a result of deformation rather than morphology and growth during life.

Finally, the linear regressions do not appear to plateau despite the wide size range (*c.* 5–50 mm). This raises the question of whether there was a maximum size of *Eoandromeda* or whether they had indeterminate growth. Many aquatic soft-bodied invertebrates, such as coelenterates, echinoderms, annelids, molluscs and urochordates, show indeterminate growth and can vary greatly in growth rate, final size and response to environmental conditions (Sebens 1987). The ecological benefit to this growth plan is the facilitation of continuous increased feeding rate and reproductive output without an increased energy investment in growth (Lord & Shanks 2012). Whether *Eoandromeda* grew continuously is unknown; it was nevertheless capable of substantial growth.

Evidence for benthic life mode

There are three conflicting hypotheses regarding *Eoandromeda*'s life mode: benthic (Zhu *et al.* 2008), pelagic (Tang *et al.* 2011a), and pelagic as a 'juvenile' to mostly benthic as an 'adult' (Wang *et al.* 2020). Expanding upon the most recent hypothesis; Wang *et al.* (2020) proposed that the lack of preserved 'juvenile' specimens, the disproportionate increase of arm thickness and rigidity to body size in their preserved specimens and the presence of 'feather-like lamellae' and 'skirts' suggested an actively swimming (pelagic) 'juvenile' stage, followed by mostly benthic 'adult' and 'senescent' stages.

The suggestion of an actively swimming 'juvenile' stage is not supported by the results from this dataset. The '-feather-like lamellae' and 'skirts' are absent from all South Australian specimens, and even in some of the figured Chinese specimens (Zhu *et al.* 2008, fig. 1A–F, I; Tang *et al.* 2011a, fig. 1L). The absence of these features offers

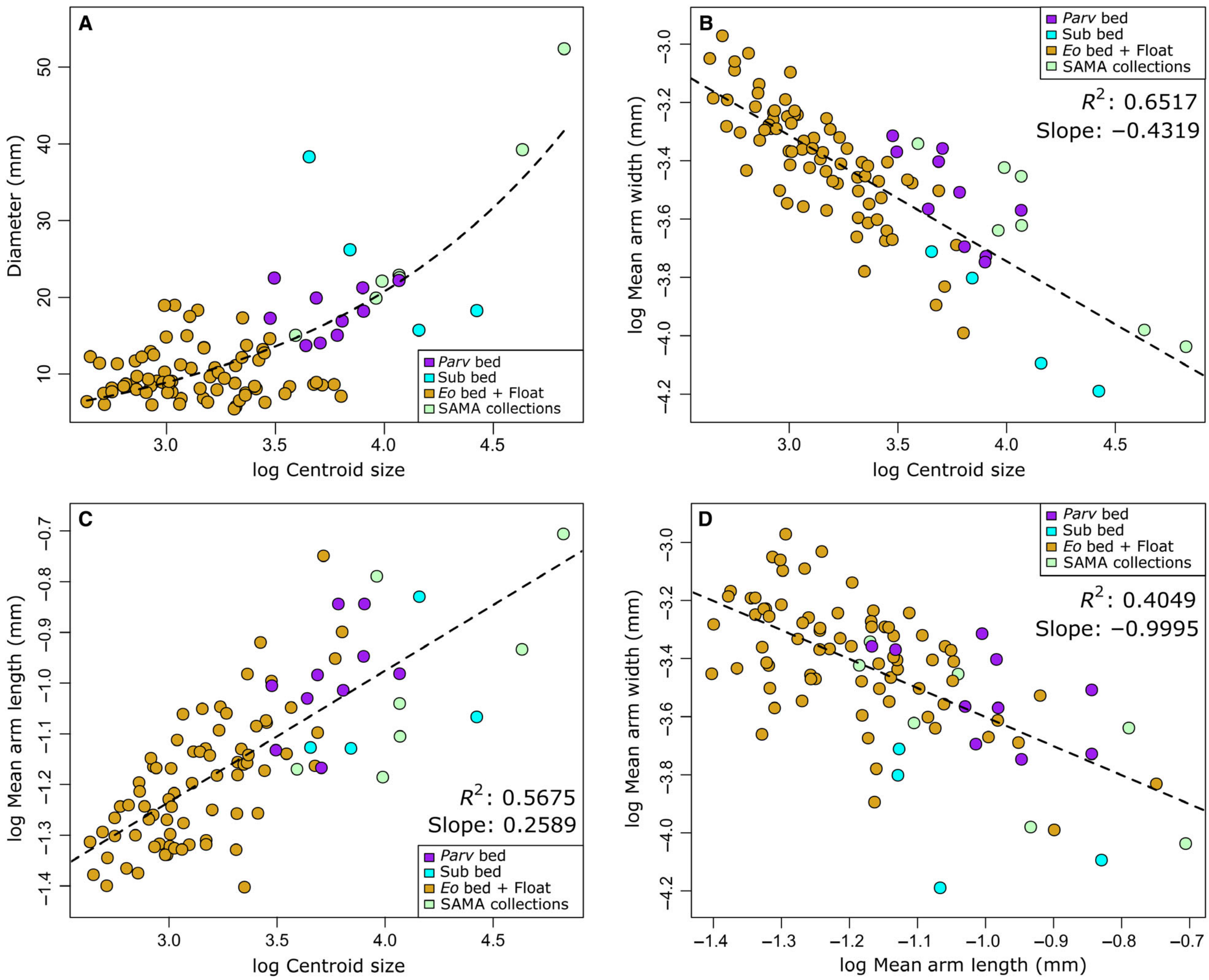

FIG. 5. Linear regressions of *Eoandromeda octobrachiata*. A, log centroid size vs diameter (mm) (for comparison/context). B, log centroid size vs log mean arm width (mm). C, log centroid size vs log mean arm length (mm). D, log mean arm length vs log mean arm width (mm). Complementary to multivariate regression (looking at different aspects of growth that landmarks do not capture, directly testing the analyses of Wang *et al.* 2020).

more support to a benthic hypothesis rather than active swimming. However, it is not certain whether the lack of these features is due to preservational differences or whether it is a true absence. Comparisons between smaller specimens from both taphonomic windows are not possible given that there are no specimens <10 mm found in China. All *c.* 200 specimens consistently rotate in an anticlockwise direction in the beds and no specimens were upside down or completely on the side (only deformation to one side in a current). This is not consistent with a pelagic mode of life because specimens would have been pulled from the water column during the burial events and have multiple orientations and oblique compaction angles and be less likely to be preserved, as is the case of unequivocal pelagic soft-bodied organisms in the Cambrian (Conway Morris & Collins 1996; Cartwright *et al.* 2007; Han *et al.* 2016). Additionally, the orientation of specimen deformation in accordance with the burial current on two beds also does not suggest a pelagic lifestyle. Ediacara taxa that are mobile or pelagic (i.e. *Dickinsonia*, *Attenborites* and *Kimberella*) tend to have very distinct and crisp edges while sessile, benthic taxa do not (Darroch *et al.* 2017; Evans *et al.* 2019; Droser *et al.* 2020). Although *Eoandromeda* has distinct arms, the edge of the specimens is not distinct and tends to fade into the texture of the mat. This is especially apparent on the WS-Sub bed, which has the most mature microbial mat of the three beds, and the specimens have a more ‘mangled’ appearance (Fig. 2E). Moreover, the abundance of ‘juvenile’ specimens in our dataset, the lack of significant shape changes with size, and the decrease of arm width with body size do not support the Wang *et al.* (2020)

hypothesis but rather the hypothesis from Zhu *et al.* (2008) of a fully benthic mode of life.

Also, the spiralling of the arms could have manipulated water flow to aid in feeding. There has been a growing list of Ediacaran organisms that are hypothesized to have influenced water flow dynamics for benthic suspension feeding (Penny *et al.* 2014; Rahman *et al.* 2015; Wood & Curtis 2015; Gibson *et al.* 2019; Cracknell *et al.* 2021) and osmotrophic life habits (Singer *et al.* 2012). Specifically, in the White Sea assemblage, fluid dynamics studies on radial organisms *Tribrachidium heraldicum* (Rahman, *et al.* 2015) and *Arkarua adami* (Cracknell, *et al.* 2021), found that their morphology slowed and redirected water flow to specific structures, consistent with passive suspension feeding through gravitational settling. This feeding strategy has been inferred to become more widespread in the White Sea assemblage from the predominantly osmotrophic fronds of the Avalon assemblage (Laflamme *et al.* 2009; Hoyal Cuthill & Conway Morris 2014; Liu *et al.* 2015), becoming the feeding strategy for 'reefs' in the Nama assemblage (Penny *et al.* 2014; Wood & Curtis 2015). Modern invertebrates such as coral (Johnson & Sebens 1993), zoanthids (Koehl 1977), oysters (Bernard 1974) and crinoids (Meyer 1979) have also been reported to utilize passive suspension feeding. Additionally, ridges and grooves in an organism's body plan often relate to their mode of life. Differences in the shell ridges of extant scallops are observed depending on which ecological niche they exploit (i.e. boring, gliding, cementing, nestling, byssal-attaching and free-living) (Stanley 1988; Morton & Thurston 1989; Morton 1996; Serb *et al.* 2011; Dinesen & Morton 2014; Sherratt *et al.* 2017). For example, burrowing scallops often have asymmetric sculptural features that aid in gripping sediment during burial (Stanley 1988). Given the apparent widespread utilization of the passive suspension feeding strategy in the White Sea assemblage, the similarity in structure to both *Tribrachidium* and *Arkarua*, and the fact that ridges are often related to function, it is reasonable to suggest that the function of *Eoandromeda*'s structure could have been to redirect and slow water flow to facilitate this type of feeding.

Ctenophore hypothesis

In association with the pelagic hypothesis, Tang *et al.* (2011a) proposed that *Eoandromeda* was a stem-group ctenophore based on morphological similarities to extant taxa of this phylum. Tang *et al.* (2011a) compared transverse bands along the arms to ctenes, the eight arms were related to the eight comb rows, and the apparent tubular structure of the arms interpreted as eight meridional canals. The central structure of *Eoandromeda* was interpreted to be the aboral ring because it resembles the shape, size and position of those seen in the Cambrian ctenophores (Conway Morris & Collins 1996). However, there are various morphological and ecological aspects that are not consistent with the Ctenophora lineage.

First, *Eoandromeda* is found on several fossil beds unlike the sparse fossil record of ctenophores, which consists of a handful of specimens in the Cambrian and Devonian (Stanley & Stürmer 1983; Conway Morris & Collins 1996; Hu *et al.* 2007; Ou *et al.* 2015; Klug *et al.* 2021). This is consistent with a benthic lifestyle for *Eoandromeda* because pelagic organisms are less commonly preserved. For example, *Attenborites* is found in large numbers but occurs only on a single bed (Droser *et al.* 2020), which is consistent with the preservation of known pelagic organisms, such as jellyfish (Cartwright *et al.* 2007). There are proposed benthic ctenophores from the Cambrian (Conway Morris 1978; O'Brien & Caron 2012; Kimmig *et al.* 2017; Zhao *et al.* 2019; Parry *et al.* 2021), however, these are debated (Ou *et al.* 2015; Zhao *et al.* 2019; Klug *et al.* 2021; Parry *et al.* 2021) and phylogenetic analyses generally support a pelagic ancestor (Jékely *et al.* 2015; Alamaru *et al.* 2017).

Furthermore, although *Eoandromeda* has some morphological similarities to extant ctenophores, they bear little resemblance to Cambrian ctenophores. Proposed Cambrian ctenophores include the benthic sea-anemone-like taxa *Xianguangia* (Chen & Erdtmann 1991), *Daihua* (Zhao *et al.* 2019), and stalked taxa *Siphusauctum* (O'Brien & Caron 2012) and *Dinomischus* (Conway Morris 1978). Although the exact positioning of the individual taxa is debated (Ou *et al.* 2015; Zhao *et al.* 2019; Klug *et al.* 2021; Parry *et al.* 2021), these are typically placed as stem lineages before the more definitive pelagic Cambrian ctenophores, which have numerous comb rows (24 and greater) and globose body shapes (Conway Morris & Collins 1996; Ou *et al.* 2015). The addition of *Eoandromeda* to this complicated evolutionary story would require that ctenophores began somewhat morphologically similar to extant pelagic ctenophores with a spiral arrangement. Rapid evolution produced more complex benthic forms in the early Cambrian, and by the middle Cambrian they had evolved into complex pelagic forms with numerous comb rows. By the Devonian, taxa start to have more crown-group morphology (Stanley & Stürmer 1983; Klug *et al.* 2021), leading to the forms extant today (to which *Eoandromeda* is most morphologically similar), with a small, morphologically simplistic, motile, benthic lineage (Alamaru *et al.* 2016; Alamaru *et al.* 2017; Glynn *et al.* 2017) secondarily evolving from a pelagic ancestor (Moroz *et al.* 2014; Whelan *et al.* 2017). This placement is not parsimonious, and requires a complicated and quick evolution involving major anatomical shifts (with and without the presence of the problematic benthic Cambrian ctenophores) (Daley & Antcliffe 2019). Taking this into consideration, it is unlikely that *Eoandromeda* is a representative of a stem-group ctenophore (Zhao *et al.* 2019). Rather, *Eoandromeda* could simply be a representative of early diploblastic organisms (Zhu *et al.* 2008).

CONCLUSION

Our study provides strong evidence that places *Eoandromeda* down on the sea floor as a benthic, sessile, radially symmetrical organism that was possibly cone shaped. The present results suggest that *Eoandromeda* was highly susceptible to deformation in accordance with burial conditions and therefore most probably consisted of a more flexible material and/or was fluid filled. We observed varying allometric relationships for the different morphological features, which suggest that the arms grew in a spiral, creating larger specimens that appear more tightly coiled than smaller ones. Together our results do not support the stem-group ctenophore hypothesis (despite some superficial morphological similarities), therefore it remains unknown as to where *Eoandromeda* fits into the tree of life. However, aforementioned proposed ecological and morphological traits bear a striking likeness to processes still widely utilized by marine organisms today, demonstrating the early evolution of common modern traits and the complexity of the Ediacara biota.

Acknowledgements. We acknowledge that the Flinders Ranges lie in the traditional lands of the Adnyamathanha people and pay our respect to their Elders past, present and emerging. We thank Jane and Ross Fargher and the Department of Environment and Water (permit to DCGB: Q27112-1) for access to the fossils at Nilpena Ediacara National Park. Funding was received from the University of Adelaide Student Support Fund, N. Gary Lane Student Research Award (Paleontological Society) and NASA Exobiology Grants (18-EXO18-0096 and 20-EXO20-0009 to MLD and DCGB) and ARC Discovery Project Grant (DP220102772 to DCGB and MLD). DCGB and ES were supported by Australian Research Council Future Fellowships (FT130101329 and FT190100803, respectively). We also thank Dr Sarbin Ranjitkar for lending the intraoral scanner to TLB and DCGB for additional data collection; the SAMA Palaeontological Manager Dr Mary-Anne Binnie for providing access to specimens in the collections; Yoland Savriama and Sylvian Gerber for help troubleshooting during the morphometrics analysis; C and T Ireland, M-A Binnie, I Hughes, S Evans and R Surprenant for help and guidance in the field; and P. Dzaugis, M. Dzaugis, S. Evans and I. Hughes for excavation of the LV-Eo bed. Open access publishing facilitated by The University of Adelaide, as part of the Wiley - The University of Adelaide agreement via the Council of Australian University Librarians.

Author contributions. **Conceptualization** TL Botha (TLB); **Data Curation** TLB, ML Droser (MLD), JG Gehling (JGG); **Formal Analysis** TLB; **Funding Acquisition** TLB, MLD, E Sherratt (ES), DC García-Bellido (DCGB); **Investigation** TLB; **Methodology** TLB, ES; **Project Administration** TLB; **Resources** ES, MLD, DCGB; **Software** TLB, ES; **Supervision** ES, MLD, DCGB; **Validation** TLB, ES, MLD, DCGB; **Visualization** TLB; **Writing – Original Draft Preparation** TLB; **Writing – Review & Editing** TLB, ES, MLD, DCGB.

DATA ARCHIVING STATEMENT

Data for this study, including the landmark files, R code (and associated functions) and raw measurements, are available in the Dryad Digital Repository: https://doi.org/10.5061/dryad.2jm63xsvg. Scan data for this study are available in FigShare: https://doi.org/10.25909/23528958.

Editor. Imran Rahman

SUPPORTING INFORMATION

Additional Supporting Information can be found online (https://doi.org/10.1002/spp2.1530):

Fig. S1. Arm width analysis of *Eoandromeda* WS-Parv bed 152S 576E.
Fig. S2. Categorizing of *Eoandromeda* offsetting of both complete and incomplete specimens.
Fig. S3. Morphospace of all landmarked *Eoandromeda* specimens.
Fig. S4. Multivariate regression of *Eoandromeda* separated by fossil bed.
Table S1. Multivariate regression of asymmetric shape components with size.

REFERENCES

ADAMS, D., COLLYER, M. and KALIONTZOPOULOU, A. 2021. geomorph: software for geometric morphometric analyses. R package v4.0. https://cran.r-project.org/web/packages/geomorph/index.html

ALAMARU, A., BROKOVICH, E. and LOYA, Y. 2016. Four new species and three new records of benthic ctenophores (Family: Coeloplanidae) from the Red Sea. *Marine Biodiversity*, **46**, 261–279.

ALAMARU, A., HOEKSEMA, B. W., van der MEIJ, S. E. T. and HUCHON, D. 2017. Molecular diversity of benthic ctenophores (Coeloplanidae). *Scientific Reports*, **7**, 6365.

BERNARD, F. R. 1974. Particle sorting and labial pulp function in the Pacific oyster Crassostrea gigas (Thunberg, 1795). *The Biological Bulletin*, **146**, 1–10.

BOOKSTEIN, F. L. 1991. Distance measures. 88–124. Bookstein, F. L. *Morphometric tools for landmark data*. Cambridge University Press.

CARTWRIGHT, P., HALGEDAHL, S., HENDRICKS, J., JARRARD, R., MARQUES, A., COLLINS, A. and LIEBERMAN, B. 2007. Exceptionally preserved jellyfishes from the middle Cambrian. *PLoS One*, **2**, e1121.

CHEN, J.-Y. and ERDTMANN, B. D. 1991. Lower Cambrian fossil Lagerstatte from Chengjiang, Yunnan, China: insights for reconstructing early metazoan life. 57–78. *In* SIMONETTA, A. M. and CONWAY MORRIS, S. (eds) *The early evolution of Metazoa and the significance of problematic taxa*. Cambridge University Press.

CIGNONI, P., CALLIERI, M., CORSINI, M., DELLEPIANE, M., GANOVELLI, F. and RANZUGLIA, G. 2008. MeshLab: an open-source mesh processing tool. 129–136. *In* SCARANO, V., de CHIARA, R. and ERRA, U. (eds) *Eurographics Italian Chapter Conference*. The Eurographics Association.

CLAUDE, J. 2013. Log-shape ratios, Procrustes superimposition, elliptical Fourier analysis: three worked examples in R. *Hystrix*, **24**, 94–102.

CONWAY MORRIS, S. 1978. A new entoproct-like organism from the Burgess Shale of British Columbia. *Palaeontology*, **20**, 833–845.

CONWAY MORRIS, S. and COLLINS, D. H. 1996. Middle Cambrian ctenophores from the Stephen Formation, British Columbia, Canada. *Philosophical Transactions of the Royal Society B*, **351**, 279–308.

COUTTS, F. J., GEHLING, J. G. and GARCÍA-BELLIDO, D. C. 2016. How diverse were early animal communities? An example from Ediacara Conservation Park, Flinders Ranges, South Australia. *Alcheringa*, **40**, 407–421.

COHEN, K. M., FINNEY, S. C., GIBBARD, P. L. and FAN, J. X. 2013; updated. The ICS International Chronostratigraphic Chart. *Episodes*, **36**, 199–204.

CRACKNELL, K., GARCÍA-BELLIDO, D. C., GEHLING, J. G., ANKOR, M. J., DARROCH, S. A. F. and RAHMAN, I. A. 2021. Pentaradial eukaryote suggests expansion of suspension feeding in White Sea-aged Ediacaran communities. *Scientific Reports*, **11**, 4121.

CUNNINGHAM, J. A., LIU, A. G., BENGSTON, S. and DONOGHUE, P. C. J. 2016. The origin of animals: can molecular clocks and the fossil record be reconciled? *BioEssays*, **39**, 1–12.

DALEY, A. C. and ANTCLIFFE, J. B. 2019. Evolution: the battle of the first animals. *Current Biology*, **29**, R257–R259.

DARROCH, S. A. F., RAHMAN, I. A., GIBSON, B., RACICOT, R. A. and LAFLAMME, M. 2017. Inference of facultative mobility in the enigmatic Ediacaran organism *Parvancorina*. *Biology Letters*, **13**, 2017033.

DINESEN, G. E. and MORTON, B. 2014. Review of the functional morphology, biology and perturbation impacts on the boreal, habitat-forming horse mussel *Modiolus modiolus* (Bivalvia: Mytilidae: Modiolinae). *Marine Biology Research*, **10**, 845–870.

DING, L., LI, Y., HU, X., XIAO, Y., SU, C.-Q. and HUANG, J. 1996. *Sinian Miaohe biota*. Geological Publishing House, Beijing, 221 pp.

DROSER, M. L. and GEHLING, J. G. 2015. The advent of animals: the view from the Ediacaran. *Proceedings of the National Academy of Sciences*, **112**, 4865–4870.

DROSER, M. L., TARHAN, L. G. and GEHLING, J. G. 2017. The rise of animals in a changing environment: global ecological innovation in the late Ediacaran. *Annual Review of Earth & Planetary Sciences*, **45**, 593–617.

DROSER, M. L., GEHLING, J. G., TARHAN, L. G., EVANS, S. D., HALL, C. M. S., HUGHES, I. V., HUGHES, E. B., DZAUGIS, M. E., DZAUGIS, M. P., DZAUGIS, P. W. and RICE, D. 2019. Piecing together the puzzle of the Ediacara Biota: excavation and reconstruction at the Ediacara National Heritage site Nilpena (South Australia). *Palaeogeography, Palaeoclimatology, Palaeoecology*, **513**, 132–145.

DROSER, M. L., EVANS, S. D., DZAUGIS, P. W., HUGHES, E. B. and GEHLING, J. G. 2020. *Attenborites janeae*: a new enigmatic organism from the Ediacara Member (Rawnsley Quartzite), South Australia. *Australian Journal of Earth Sciences*, **67**, 915–921.

DROSER, M. L., EVANS, S. D., TARHAN, L. G., SURPRENANT, R. L., HUGHES, I. V., HUGHES, E. B. and GEHLING, J. G. 2022. What happens between depositional events, stays between depositional events: the significance of organic mat surfaces in the capture of Ediacara communities and the sedimentary rocks that preserve them. *Frontiers in Earth Science*, **10**, 1–10.

DRYDEN, I. L. 2019. shapes: statistical shape analysis. R package v1.2.5. https://cran.r-project.org/web/packages/shapes/index.html

EVANS, S. D., GEHLING, J. G. and DROSER, M. L. 2019. Slime travelers: early evidence of animal mobility and feeding in an organic mat world. *Geobiology*, **17**, 490–509.

GEHLING, J. G. 2000. Environmental interpretation and a sequence stratigraphic framework for the terminal Proterozoic Ediacara Member within the Rawnsley Quartzite, South Australia. *Precambrian Research*, **100**, 65–95.

GEHLING, J. G. and DROSER, M. L. 2012. Ediacaran stratigraphy and the biota of the Adelaide Geosyncline, South Australia. *Episodes*, **35**, 236–246.

GEHLING, J. G. and DROSER, M. L. 2013. How well do fossil assemblages of the Ediacara Biota tell time? *Geology*, **41**, 447–450.

GEHLING, J. G., GARCÍA-BELLIDO, D. C., DROSER, M. L., TARHAN, M. L. and RUNNEGAR, B. 2019. The Ediacaran–Cambrian transition: sedimentary facies versus extinction. *Estudios Geológicos*, **75**, e099.

GIBSON, B. M., RAHMAN, I. A., MALONEY, K. M., RACICOT, R. A., MOCKE, H., LAFLAMME, M. and DARROCH, S. A. F. 2019. Gregarious suspension feeding in a modular Ediacaran organism. *Science Advances*, **5**, eaaw0260.

GLYNN, P. W., COFFMAN, B., FULLER, M. P. C., MOORHEAD, S. G., WILLIAMS, M. K., PRIMOV, K. D., FORTSON, T. N., BARRALES, R. N. and GLYNN, P. J. 2017. Benthic ctenophores (Platyctenida: Coeloplanidae) in south Florida: environmental conditions, habitats, abundances, and behaviors. *Invertebrate Biology*, **136**, 379–393.

GOULD, S. J. 1966. Allometry and size in ontogeny and phylogeny. *Biological Reviews*, **41**, 587–640.

HAN, J., HU, S., CARTWRIGHT, P., ZHAO, F., OU, Q., KUBOTA, S., WANG, X. and YANG, X. 2016. The earliest pelagic jellyfish with rhopalia from Cambrian Chengjiang Lagerstätte. *Palaeogeography, Palaeoclimatology, Palaeoecology*, **449**, 166–173.

HOLLO, G. 2015. A new paradigm for animal symmetry. *Interface Focus*, **5**, 20150032.

HOYAL CUTHILL, J. F. and CONWAY MORRIS, S. 2014. Fractal branching organizations of Ediacaran rangeomorph fronds reveal a lost Proterozoic body plan. *Proceedings of the National Academy of Sciences*, **111**, 13122–13126.

HU, S., STEINER, M., ZHU, M., ERDTMANN, B. D., LUO, H., CHEN, L. and WEBER, B. 2007. Diverse pelagic predators from the Chengjiang Lagerstatte and the establishment of modern-style pelagic ecosystems in the early Cambrian. *Palaeogeography, Palaeoclimatology, Palaeoecology*, **254**, 307–316.

HUXLEY, J. S. and TEISSIERR, G. 1936. Terminology of relative growth. *Nature*, **137**, 780–781.

JÉKELY, G., PAPS, J. and NIELSEN, C. 2015. The phylogenetic position of ctenophores and the origin(s) of nervous systems. *EvoDevo*, **6**, 1.

JOHNSON, A. S. and SEBENS, K. P. 1993. Consequences of a flattened morphology: effects of flow on feeding rates of the scleractinian coral *Meandrina meandrites*. *Marine Ecology Progress Series*, **99**, 99–114.

KIMMIG, J., STROTZ, L. C. and LIEBERMAN, B. S. 2017. The stalked filter feeder *Siphusauctum lloydguntheri* n. sp. From the middle Cambrian (Series 3, Stage 5) Spence Shale of Utah: its biological affinities and taphonomy. *Journal of Paleontology*, **91**, 902–910.

KLINGENBERG, C. P. 2016. Size, shape, and form: concepts of allometry in geometric morphometrics. *Development Genes & Evolution*, **226**, 113–137.

KLUG, C., KERR, J., LEE, M. S. Y. and CLOUTIER, R. 2021. A late-surviving stem-ctenophore from the Late Devonian of Miguasha (Canada). *Scientific Reports*, **11**, 19039.

KOEHL, M. A. R. 1977. Water flow and the morphology of zoanthid colonies. 437–444. *In* TAYLOR, D. L. (ed.) *Proceedings, Third International Coral Reef Symposium*. University of Miami.

LAFLAMME, M., XIAO, S. and KOWALEWSKI, M. 2009. Osmotrophy in modular Ediacara organisms. *Proceedings of the National Academy of Sciences*, **106**, 14438–14443.

LIU, A. G., KENCHINGTON, C. G. and MITCHELL, E. G. 2015. Remarkable insights into the paleoecology of the Avalonian Ediacaran macrobiota. *Gondwana Research*, **27**, 1355–1380.

LORD, J. P. and SHANKS, A. L. 2012. Continuous growth facilitates feeding and reproduction: impact of size on energy allocation patterns for organisms with indeterminate growth. *Marine Biology*, **159**, 1417–1428.

LOY, A., MARIANI, L., BERTELLETTI, M. and TUNESI, L. 1998. Visualizing allometry: geometric morphometrics in the study of shape changes in the early stages of the two-banded sea bream, *Diplodus vulgaris* (Perciformes, Sparidae). *Journal of Morphology*, **237**, 137–146.

MACGABHANN, B. A. 2014. There is no such thing as the 'Ediacara Biota'. *Geoscience Frontiers*, **5**, 53–62.

MANUEL, M. 2009. Early evolution of symmetry and polarity in metazoan body plans. *Comptes Rendus Biologies*, **332**, 184–209.

MARTIN, M. W., GRAZHDANKIN, D. V., BOWRING, S. A., EVANS, D. A. D., FEDONKIN, M. A. and KIRSCHVINK, J. L. 2000. Age of Neoproterozoic bilatarian body and trace fossils, White Sea, Russia: implications for Metazoan evolution. *Science*, **288**, 841–845.

MEYER, D. L. 1979. Length and spacing of the tube feet in Crinoids (Echinodermata) and their role in suspension-feeding. *Marine Biology*, **51**, 361–369.

MITTEROECKER, P. and GUNZ, P. 2009. Advances in geometric morphometrics. *Evolutionary Biology*, **36**, 235–247.

MONTEIRO, L. R. 1999. Multivariate regression models and geometric morphometrics: the search for causal factors in the analysis of shape. *Systematic Biology*, **48**, 192–199.

MOROZ, L. L., KOCOT, K. M., CITARELLA, M. R., DOSUNG, S., NOREKIAN, T. P., POVOLOTSKAYA, I. S., GRIGORENKO, A. P., DAILEY, C., BEREZIKOV, E., BUCKLEY, K. M., PTITSYN, A., RESHETOV, D., MUKHERJEE, K., MOROZ, T. P., BOBKOVA, Y., YU, F., KAPITONOV, V. V., JURKA, J., BOBKOV, Y. V., SWORE, J. J., GIRARDO, D. O., FODOR, A., GUSEV, F., SANFORD, R., BRUDERS, R., KITTLER, E., MILLS, C. E., RAST, J. P., DERELLE, R., SOLOVYEV, V. V., KONDRASHOV, F. A., SWALLA, B. J., SWEEDLER, J. V., ROGAEV, E. I., HALANYCH, K. M. and KOHN, A. B. 2014. The ctenophore genome and the evolutionary origins of neural systems. *Nature*, **510**, 109–138.

MORTON, B. 1996. The biology and functional morphology of *Minnivola pyxidatus* (Bivalvia: Pectinoidea). *Journal of Zoology*, **240**, 735–760.

MORTON, B. and THURSTON, M. H. 1989. The functional morphology of *Propeamussium lucidurn* (Bivalvia: Pectinacea), a deep-sea predatory scallop. *Journal of Zoology*, **218**, 471–496.

MOSIMANN, J. E. 1970. Size allometry: size and shape variables with characterizations of the lognormal and generalized gamma distributions. *Journal of the American Statistical Association*, **65**, 930–945.

NARBONNE, G. M., XIAO, S., SHIELDS, G. A. and GEHLING, J. G. 2012. The Ediacaran period. 413–435. *In* GRADSTEIN, F., OGG, J. G., SCHMITZ, M. D. and OGG, G. M. (eds) *The geologic time scale 2012*. Elsevier.

O'BRIEN, L. J. and CARON, J. B. 2012. A new stalked filter-feeder from the middle Cambrian Burgess Shale, British Columbia, Canada. *PLoS One*, **7**, e29233.

OU, Q., XIAO, S., HAN, J., SUN, G., ZHANG, F., ZHANG, Z. and SHU, D. 2015. A vanished history of skeletonization in Cambrian comb jellies. *Science Advances*, **1**, e1500092.

PARRY, L. A., LEROSEY-AUBRIL, R., WEAVER, J. C. and ORTEGA-HERNANDEZ, J. 2021. Cambrian comb jellies from Utah illuminate the early evolution of nervous and sensory systems in ctenophores. *iScience*, **24**, 102943.

PATERSON, J. R., GEHLING, J. G., DROSER, M. L. and BICKNELL, R. D. C. 2017. Rheotaxis in the Ediacaran epibenthic organism *Parvancorina* from South Australia. *Scientific Reports*, **7**, 45539.

PENNY, A. M., WOOD, R., CURTIS, A., BOWYER, F., TOSTEVIN, R. and HOFFMAN, K. H. 2014. Ediacaran metazoan reefs from the Nama Group, Namibia. *Science*, **344**, 1504–1506.

PLATE, T. and HEIBERGER, R. 2016. abind: combine multidimensional arrays. R package v1.4-5. https://cran.r-project.org/web/packages/abind/index.html

PREISS, W. V. 2000. The Adelaide Geosyncline of South Australia and its significance in Neoproterozoic continental reconstruction. *Precambrian Research*, **100**, 21–63.

R CORE TEAM. 2013. R: a language and environment for statistical computing. R Foundation for Statistical Computing. https://www.r-project.org/

RAHMAN, I. A., DARROCH, S. A. F., RACICOT, R. A. and LAFLAMME, M. 2015. Suspension feeding in the enigmatic Ediacaran organism *Tribrachidium* demonstrates complexity of Neoproterozoic ecosystems. *Science Advances*, **1**, e1500800.

ROHLF, F. J. and SLICE, D. E. 1990. Extensions of the Procrustes method for the optimal superimposition of landmarks. *Systematic Zoology*, **39**, 40–59.

SAVRIAMA, Y. 2018. A step-by-step guide for geometric morphometrics of floral symmetry. *Frontiers in Plant Science*, **9**, 1433.

SCHLAGER, S. 2017. Morpho and Rvcg: shape analysis in R. 217–256. *In* ZHENG, G., LI, S. and GABOR, S. (eds) *Statistical shape and deformation analysis*. Academic Press.

SEBENS, K. P. 1987. The ecology of indeterminate growth in animals. *Annual Review of Ecology & Systematics*, **18**, 371–407.

SERB, J. M., ALEJANDRINO, A., OTÁROLA-CASTILLO, E. and ADAMS, D. C. 2011. Morphological convergence of shell shape in distantly related scallop species (Mollusca: Pectinidae). *Zoological Journal of the Linnean Society*, **163**, 571–584.

SHERRATT, E., SERB, J. M. and ADAMS, D. C. 2017. Rates of morphological evolution, asymmetry and morphological integration of shell shape in scallops. *BMC Evolutionary Biology*, **17**, 248.

SINGER, A., PLOTNICK, R. and LAFLAMME, M. 2012. Experimental fluid mechanics of an Ediacaran frond. *Palaeontologia Electronica*, **15** (2), 19A.

STANLEY, S. M. 1988. Adaptive morphology of the shell in bivalves and gastropods. *The Mollusca*, **11**, 105–141.

STANLEY, G. D. Jr and STÜRMER, W. 1983. The first fossil ctenophore from the Lower Devonian of West Germany. *Nature*, **303**, 518–520.

TANG, F. 2012. *Eoandromeda octobrachiata* and the evolution of early animals. *Acta Geoscientica Sinica*, **33**, 721–729. [in Chinese with English abstract]

TANG, F., YIN, C., BENGTSON, S., LIU, P., WANG, Z. and GAO, L. 2008. Octoradiate spiral organisms in the Ediacaran of South China. *Acta Geologica Sinica*, **82**, 27–34.

TANG, F., YIN, C., BENGTSON, S., LIU, P., WANG, Z., CHEN, S. and GAO, L. 2009. The Ediacaran ctenophore (*Eoandromeda octobrachiata*) from South China. *Acta Geoscientica Sinica*, **30**, 543–553. [in Chinese with English abstract]

TANG, F., BENGTSON, S., WANG, Y., WANG, X. and YIN, C. 2011a. *Eoandromeda* and the origin of Ctenophora. *Evolution & Development*, **13**, 408–414.

TANG, F., BENGTSON, S., YIN, C.-Y. and GAO, L.-Z. 2011b. New data of *Eoandromeda octobrachiata* and their indications. *Acta Geoscientica Sinica*, **32**, 641–651. [in Chinese with English abstract]

TARHAN, L., DROSER, M., GEHLING, J. and DZAUGIS, M. 2017. Microbial mat sandwiches and other anactualistic sedimentary features of the Ediacara Member (Rawnsley Quartzite, South Australia): implications for interpretation of the Ediacaran sedimentary record. *PALAIOS*, **32**, 181–194.

TURNER, A. M., DELEAN, S. and GARCÍA-BELLIDO, D. C. 2021. Preliminary revision of the morphology of *Phyllozoon hanseni* from the Ediacaran of South Australia. *Serie Correlación Geológica*, **37**, 5–14.

WANG, Y., WANG, Y., TANG, F., ZHAO, M. and LIU, P. 2020. Lifestyle of the octoradiate *Eoandromeda* in the Ediacaran. *Paleontological Research*, **24**, 1.

WHELAN, N. V., KOCOT, K. M., MOROZ, T. P., MUKHERJEE, K., WILLIAMS, P., PAULAY, G., MOROZ, L. L. and HALANYCH, K. M. 2017. Ctenophore relationships and their placement as the sister group to all other animals. *Nature Ecology & Evolution*, **1**, 1737–1746.

WICKHAM, H. 2016. *ggplot2: Elegant graphics for data analysis*. Springer.

WOOD, R. and CURTIS, A. 2015. Extensive metazoan reefs from the Ediacaran Nama Group, Namibia: the rise of benthic suspension feeding. *Geobiology*, **13**, 112–122.

XIAO, S., DROSER, M. L., GEHLING, J. G., HUGHES, I. V., WAN, B., CHEN, Z. and YUAN, X. 2013. Affirming life aquatic for the Ediacara biota in China and Australia. *Geology*, **41**, 1095–1098.

YIN, C.-Y., TANG, F., LIU, P.-J., GAO, L.-Z., WANG, Z.-Q. and CHEN, S.-M. 2009. New advances in the study of biostratigraphy of the Sinian (Ediacaran) Doushantuo formation in South China. *Acta Geoscientica Sinica*, **30**, 421–432. [in Chinese with English abstract]

ZHAO, Y., VINTHER, J., PARRY, L. A., WEI, F., GREEN, E., PISANI, D., HOU, X., EDGECOMBE, G. D. and CONG, P. 2019. Cambrian sessile, suspension feeding stem-group ctenophores and evolution of the comb jelly body plan. *Current Biology*, **29**, 1112–1125.

ZHOU, C., YUAN, X., XIAO, S., CHEN, Z. and HUA, H. 2018. Ediacaran integrative stratigraphy and timescale of China. *Science China Earth Sciences*, **62**, 7–24.

ZHU, M., GEHLING, J. G., XIAO, S., ZHAO, Y. and DROSER, M. L. 2008. Eight-armed Ediacara fossil preserved in contrasting taphonomic windows from China and Australia. *Geology*, **36**, 867–870.

ZHU, M. and LI, X.-H. 2017. Introduction: from snowball Earth to the Cambrian explosion – evidence from China. *Geological Magazine*, **154**, 1187–1992.